Visible light optical coherence tomography in biomedical imaging

Ji Yi[1,2,3]

(1. Department of Medicine, Boston University School of Medicine, Boston Medical Center, Boston, MA 02118;
2. Department of Biomedical Engineering, Boston University, Boston, MA 02215;
3. Department of Electric and Computer Engineering, Boston University, Boston, MA 02215)

Abstract: Optical coherence tomography (OCT) is a widely used optical imaging modality for three-dimensional structural and functional imaging. The prevalent OCT systems use an invisible light laser source beyond 800 nm and up to 1 500 nm to allow deep image penetration in biological tissues. Recently, visible light OCT (vis-OCT) using a short wavelength range between 400 nm to 700 nm has gained significant progress and attracted interest in its unique capability of high resolution imaging and spatially-resolved spectroscopy. In this article, we will briefly review the recent advance of vis-OCT imaging and its potential biomedical applications.

Key words: visible light OCT; high resolution; oximetry; spectroscopy

CLC number: R318 **Document code:** A **DOI:** 10.3788/IRLA201948.0902001

Received date: 2019-07-11; Revised date: 2019-08-21

Author: Ji Yi (1983-), male, PhD. Dr. Yi's research is focused on novel optical techniques for early disease detection, and monitoring disease progression and prognosis. Among other inventions, he developed various imaging methods that enable non-invasive detection of nanoscale structural alterations in tissue and the local oxygen metabolism. His research is at the interface of biophotonics, physics, engineering, biology and medicine, that ultimately aims to improve the health care of general public.
Email: jiyi@bu.edu

0 Introduction

Since the first demonstration in 1991, optical coherence tomography (OCT) has become one of the most widely used optical imaging techniques in biomedical researches and clinical practice [1-2]. It has fundamentally changed the standard-of-care in ophthalmology, providing unprecedented anatomical imaging in both anterior and posterior parts of the eye. It has also been actively translated into other clinical applications in dermatology, cardiology, gastroenterology, neurology, and oncology. The rapid clinical translation and technical development using OCT has created a unique and remarkable ecosystem encompassing industry, academic community and biomedicine in generating significant impacts in health care.

OCT generates non-invasive cross-sectional images within biological tissues, analogous to ultrasound imaging (UI). Instead of directly detecting the flight-of-light as in UI, OCT uses a broad-band low coherence light source and the coherence gating to discern the reflected signal from different depths. To implement the coherence gating, a Michelson interferometry is typically used to generate the interference between a reference light and the reflected light from the tissue. The relative phase delay of these two light measures the depth information. By combining a laser scanning method, a three-dimensional imaging of biological tissue can be generated in a non-destructing and non-invasive manner. Beyond the structural imaging, variety of contrasts have been harnessed for additional information. For a few examples, Doppler OCT measures the blood flow speed [3-5]. OCT angiography (OCTA) enhances the motion contrast of the blood flow to generate 3D microangiography down to the capillary level [6-8]. Polarization-sensitive OCT quantifies the birefringence in the muscle, tenders, and neural axons[9-11].

Up to date, the prevalent OCT devices use invisible near infrared (NIR) laser source beyond 800 nm and up to 1 500 nm. The imaging penetration of OCT depends on the light attenuation propagating into tissue. In the NIR wavelength range, the lower scattering from tissue and relatively weak absorption by several native absorbers creates an "optical window" that is favorable for imaging deep (Fig.1).

In the past ten years, the mature of the supercontinuum sources became commercially available that provides white light laser with a bandwidth crossing from ~400 nm to 2 000 nm and enables OCT imaging within the visible light [12]. Although the penetration depth is fundamentally shorter than NIR OCT, visible light OCT (vis-OCT) provides several its distinct advantages. First, the shorter wavelength in vis-OCT results in a better imaging resolution. Second, hemoglobin has strong absorption in the visible light rage, which allows oximetry within the microvasculature. Third, the expansion of the wavelength range enhances the capability of elastic light spectroscopy, for detecting early structural changes in diseases. In this paper, we will summarize some of the recent progress on above three features of vis-OCT and their potential biological and clinical applications.

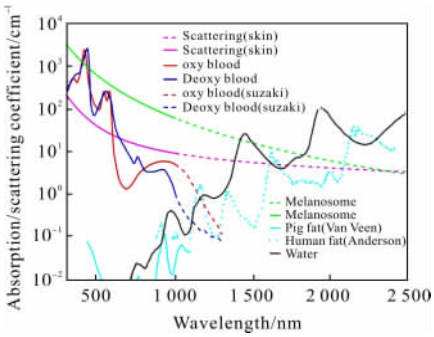

Fig.1 Absorption spectrum of intrinsic chromophores and biological tissues

1 High-resolution structural imaging by vis-OCT

OCT conventionally uses the laser scanning scheme to map the lateral plane, and the coherence gating to generate tomography. The beam width at the laser focus defines the lateral resolution σ_l,

$$\sigma_l = \frac{\lambda}{2NA} \tag{1}$$

where λ is the center wavelength of the laser, nm; and NA is the numerical aperture of the OCT imaging system.

The depth resolution σ_z determined the temporal coherence length of the laser, which can be expressed by,

$$\sigma_z = \frac{2\ln 2}{\pi}\frac{\lambda^2}{\Delta\lambda} \tag{2}$$

where $\Delta\lambda$ is the spectral width of the light source. The scaling factor considers that the spectral shape follows a Gaussian function.

It is easy to perceive that both the lateral and axial resolution can be improved by using a shorter wavelength. Povazay et al. showed for the first time the sub-micron temporal coherence length in 2003, using a femtosecond pumping laser to generate supercontinuum[13]. When applied in ophthalmology, Yi et al. showed the finer layer structures and textures in human retina in vivo, as shown in Fig.2[14]. Kho et al. and Zhang et al. further implemented the depth-dependent dispersion and applied spectral shaping, and achieved sub-micron depth resolution throughout retina[15-16]. With the shorter wavelength, the improvement of the lateral resolution is also clear [14]. In addition, adaptive optics was incorporated in vis-OCT to correct the wave front error at the imperfect optical surface, and subcellular resolution in vivo in mouse retina has been achieved[17]. Using a Bessel beam, isotropic resolutions in three dimensions were reported in resolving subcellular structures[18-21]. High resolution of vis-OCTA in mouse microvascular organization was also reported[22].

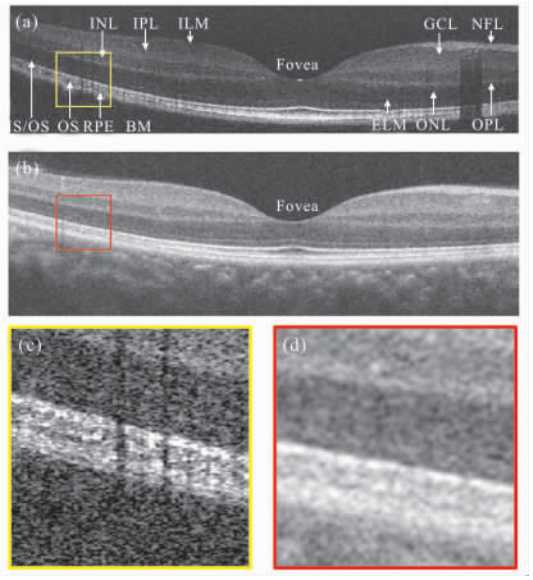

Fig.2 Visible light OCT image for human retina. (a) A representative cross-sectional vis-OCT image around the fovea. Anatomical layers include: inner limiting membrane (ILM), nerve fiber layer (NFL), ganglion cell layer (GCL), inner plexiform layer (IPL), inner nuclear layer (INL), outer plexiform layer (OPL), outer nuclear layer (ONL), inner/outer segment junction (IS/OS), outer segment of photoreceptor (OS), retinal pigmented epithelium (RPE), and Bruch's membrane (BM); (b) Corresponding image from NIR OCT; (c-d) Zoomed-in view of the box region in panel (a) and (b) showing the enhanced resolution in vis-OCT. Reprinted with the permission from Ref.[14]

2 Microvascular oximetry by vis-OCT

Hemoglobin is the major constituent within red blood cells that transports oxygen in the circulation system to maintain metabolism and biological functions. The absorption spectrum of hemoglobin is oxygenation-sensitive (Fig.1). Therefore, by a spectral analysis of blood absorption and scattering, the blood oxygen saturation (sO_2) can be quantitatively measured,

serving as an important functional biomarker. Since the absorption coefficient in visible light range is two orders of magnitudes higher than that in the NIR range, vis-OCT has much stronger oxygenation-dependent spectral contrast which is unattainable in NIR OCT due to the confounding scattering from the red blood cells[23].

OCT uses ballistic photon and coherence gating to localize the optical signal within a tissue volume. At the bottom of the vessel wall, light double-passing through the vessel lumen provides the detectable spectral contrast, which can be analytically expressed based on the Beer's law [24]

$$I(sO_2|\lambda, z)=I_0(\lambda)\sqrt{R_0 r(\lambda)}\cdot e^{-[sO_2\times\mu_{HbO_2}(\lambda)+(1+sO_2)\times\mu_{Hb}(\lambda)]z} \quad (3)$$

where $I_0(\lambda)$ is the light source's spectrum; R_0 is the reflectance of the reference arm and assumed to be a constant; $r(\lambda)$ (dimensionless) is the reflectance at the vessel wall, whose scattering spectrum can be modeled by a power law under the first Born approximation $r(\lambda)=A\lambda^{-\alpha}$ with A being a dimensionless constant and α modeling the decaying scattering spectrum from the vessel wall[25]; The optical attenuation coefficient μ (mm^{-1}) combines the absorption (μ_a) and scattering coefficients (μ_s) of the whole blood, which are both wavelength- and sO_2-dependent:

$$\mu=\mu_a+W\mu_s \quad (4)$$

where W is a scaling factor for the scattering coefficient in a range from 0 to 1[26]. The subscripts Hb and HbO_2 denote the contribution from the deoxygenated and oxygenated blood, respectively. z denotes the light penetrating depth. Then, a least square fitting method can be applied to match the experimental spectra within the vessel to the above model, to inversely estimate the sO_2.

In order to extract spectral information from the 3D images of vis-OCT, a time-frequency analysis is performed on the spectral interferogram to obtain the spatially-resolved spectra, as in spectroscopic OCT[27-28]. This spatial localization allows the isolation of the signal within the blood vessels and provides reliable sO_2 measurements, as shown in Fig.3. The feasibility of oximetry by vis-OCT was first demonstrated by Yi et al., and Roble et al. in vitro in 2010[29-30], and then in vivo in 2011 [31]. Retinal oximetry by vis-OCT was subsequently reported in 2013, expanding the potential application in ophthalmology[24]. Together with the Doppler OCT blood flow measurements, the oxygen consumption can be quantified, enabling the study of the complex physiology in the brain and the retina [32-33]. In combining OCT angiography, vis-OCTA achieved the oximetry within microvasculature down to the capillary

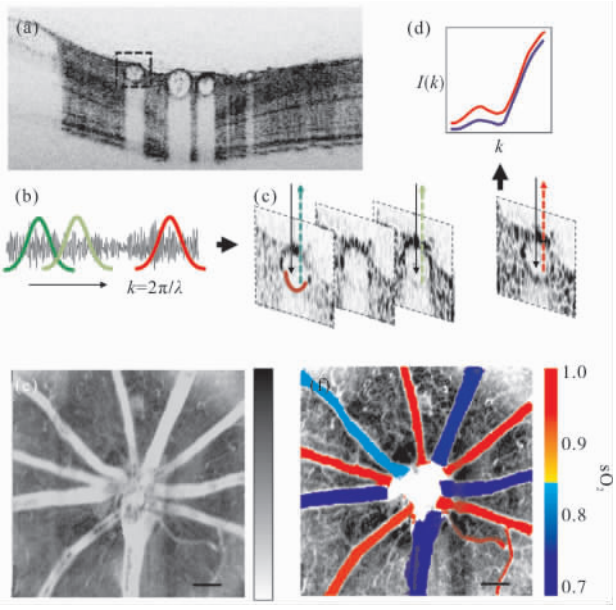

Fig.3 Illustration of vis-OCT retinal oximetry. (a) An example B-scan image of a rat retina using inversed contrast; (b), (c) By short time Fourier transform, OCT spectra from the bottom of a vessel wall were extracted. (d) Illustration of reflection spectra from artery and vein (red and blue), from which a spectral analysis can be performed to estimate sO_2. (e) En face projection of vis-OCT image on a Long Evans rat retina. (f) Fused vasculature image and sO_2 map in major vessels. Bar=200 μm. Reprinted permission from Ref. [24]

network, where the oxygen perfusion occurs [34-37]. This is a fundamental process that offers valuable insight into local biological functions. The capability of oximetry was further applied in various preclinical studies, suggesting potential clinical applications in diabetic retinopathy [38], retinopathy of prematurity [39], glaucoma [40], acute ocular hypertension[41], retinal vascular occlusion[42], stroke[43], and skin wound healing[37]. Toward the clinical translation, vis-OCT human retinal image was demonstrated in 2015 [14], and the human retinal oximetry was subsequently reported[44].

3 Scattering spectroscopy by vis-OCT

OCT detects light scattering from the tissue. The light scattering is originated from the fluctuation of the tissue refractive index [45]. According to Gladstone - Dale equation [46], the tissue refractive index, n, is linearly proportional to the local macromolecule mass density,

$$n=n_0+\rho\alpha \tag{5}$$

where ρ is the local concentration of the solid material (e.g., macromolecules), and α is the refractive index increment, usually equals to 0.17 mL/g for biological materials. n_0 is the refractive index of water. Remarkably, this relationship holds for all the major macromolecular components (e.g. protein, lipid), and thus the detection of light scattering can assess the local tissue structure. Among different methods, light scattering spectroscopy (LSS) is one major branch by analyzing the wavelength-dependent scattering signal from the tissue. A proper spectroscopic analysis can reveal the ultrastructural properties down to the length scale of several tens of nanometers[47-49]. This superb sensitivity has been already leveraged in a broad range of biomedical applications, most well-known as in early detections for cancers[50-54].

Since OCT uses a broad-band low coherence light source, there is a natural application using OCT for LSS. In comparison to NIR OCT, vis-OCT is particularly advantageous for LSS, because it has a broader wave number range in k-space with the same wavelength bandwidth. Equivalently, the short wavelength in vis-OCT provides a better sensitivity to detecting subtle tissue structural changes. By modeling the tissue structure as a statistically homogeneous media with continuous refractive index variation, the full set of tissue optical properties can be inversely calculated in vis-OCT for early detection of colorectal and pancreatic cancers[25]. Lichtenegger et al. applied the spectral analysis in a white light vis-OCT to characterize the white matter, gray matter and the neuritic amyloid-beta plaques in human Alzheimer′s disease brain samples [55]. Using the RGB components of the white light vis-OCT, a "true color" 3D reconstruction of mouse retina was reported to examine the spectral contrast in photoreceoptors, RPE, and the retinal lesion [15,56-57]. Figure 4 shows an example of using spectral analysis to quantify melanin content, an important photo-protective subcellular component in RPE. In order to obtain spectral contrasts over even a larger spectral bandwidth, dual band OCT has been developed to combine visible and NIR OCT bridging a ~300 nm wavelength range[58-59]. Song et al. developed a fiber-based visible and NIR OCT (vnOCT) system, and revealed intriguing spectral contrasts between two channels in retina (Fig.5)[60-61]. The spectral contrast in retinal nerve fiber layer was further demonstrated to be more sensitive than the anatomical changes, in detecting retinal changes potentially associated with glaucoma[40].

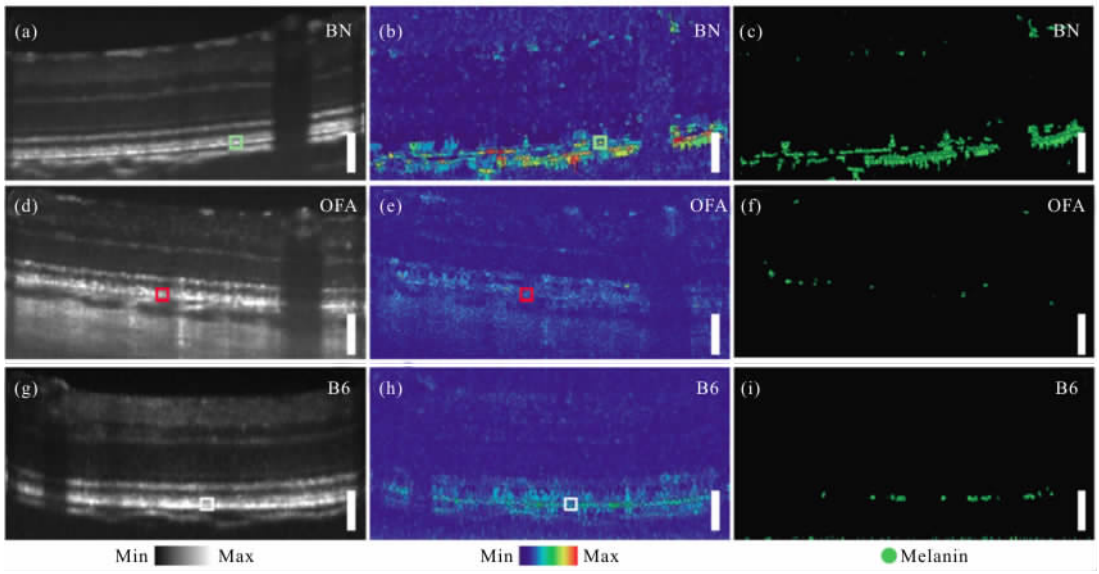

Fig.4 In vivo results of melanin visualization by hyperspectral optical coherence tomography (OCT). (a–c) Intensity, deviation from mean (DFM) and the thresholded DFM images in the Brown Norway (BN) rat retina. In the DFM plots, high signal is only observed in the retinal pigment epithelium (RPE) and the choroid, both of which are melanin–containing. (d–f) Intensity, DFM and the thresholded DFM in the albino OFA rat retina. The DFM image in (e) does not contain many pixels above the threshold (f). (g–i) Intensity, DFM and the thresholded DFM in the retina of a mouse from a C57BL/6 background (B6). The signal in the RPE is much less pronounced than in the case of the Brown Norway rat. Reprinted with permission from Ref.[56]

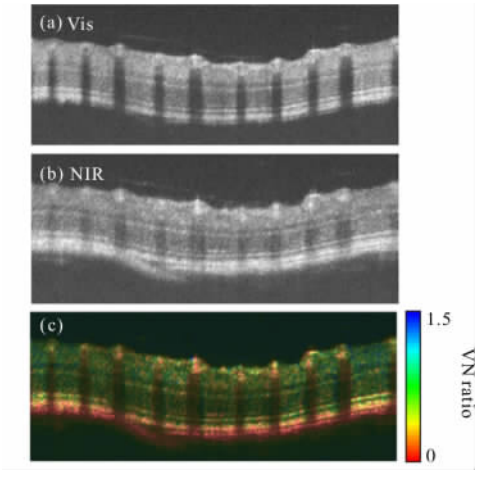

Fig.5 Spectral contrast by visible and NIR OCT (vnOCT) in mouse retina. (a–b) Circular B–scan image in visible light OCT and NIR OCT. (c) Intensity ratio between the visible and NIR channels was defined as VN ratio to quantify the spectroscopic features. Reprinted with permission from Ref.[40]

4 Summary and outlook

This review summarized the recent development of vis–OCT from instrumentation, preclinical studies and translation to human imaging for the past seven years or so. The most rapid progress occurs in ophthalmology. Multiple animal studies suggested clinical applications in all the major retinal conditions such as diabetic retinopathy, glaucoma, age–related macular degeneration and vascular occlusion. Beyond ophthalmology, as different embodiments of vis–OCT (e.g. endoscopy) develops, we should expect a continuous growth of translation from bench to bedside, and in the fundamental science as well.

As vis–OCT becomes more powerful and draws more interests, there is one major limitation that awaits to be addressed in the future. All the current vis–OCT system uses a supercontinuum laser to provide the broad–band white light source. The stochastic nature of the supercontinuum generation inherently produces the pulse–to–pulse power variation, and thus

compromises the spectral power stability. This is a major source of noise in vis-OCT, limiting the signal-to-noise ratio (SNR) and the imaging speed. In comparison, NIR OCT uses the superluminescent laser diode (SLD), and later the swept-source laser that provide much better stability, imaging SNR and speed than supercontinuum source. Both SLD and swept-source laser a re based on semiconductor manufacture technique that can be cost-effective and compact in mass production. Unfortunately, there is not yet alternative SLD and swept-source laser operating in the visible light range. What is encouraging is that there is an increasing industrial need for visible light fiber communication that would require a broad band visible light source. It is then expected that better and cheaper visible light laser sources (e.g. visible SLD) will enter the market in a foreseeable future.

In summary, we briefly reviewed the recent progress of vis-OCT and focused on three unique aspects of high resolution, oximetry, and scattering spectroscopy. Each of these three features can lead to significant biomedical applications. We anticipate that the vis-OCT will continue to emerge as a significant method in the field of biomedical imaging.

References:

[1] Huang D, Swanson E A, Lin C P, et al. Optical coherence tomography [J]. ***Science***, 1991, 254: 1178-1181.

[2] Fercher A F, Drexler W, Hitzenberger C K, et al. Optical coherence tomography -principles and applications[J]. ***Rep Prog Phys***, 2003, 66: 239-303.

[3] Leitgeb R A, Werkmeister R M, Blatter C, et al. Doppler optical coherence tomography [J]. ***Prog Retin Eye Res***, 2014, 41: 26-43.

[4] Drexler W, Fujimoto J G. Optical Coherence Tomography: Technology and Applications [M]. Berlin: Springer, 2008: 621-651.

[5] Srinivasan V J, Sakadžić S, Gorczynska I, et al. Quantitative cerebral blood flow with optical coherence tomography[J]. ***Opt Express***, 2010, 18: 2477-2494.

[6] Kashani A H, Chen C L, Gahm J K, et al. Optical coherence tomography angiography: A comprehensive review of current methods and clinical applications[J]. ***Progress in Retinal and Eye Research***, 2017, 60: 66-100.

[7] Carlo T E, Romano A, Waheed N K, et al. A review of optical coherence tomography angiography (OCTA) [J]. ***International Journal of Retina and Vitreous***, 2015, 1: 5.

[8] Baran U, Wang R K. Review of optical coherence tomography based angiography in neuroscience [J]. ***Neurophotonics***, 2016, 3: 010902.

[9] Boer J F, Hitzenberger C K, Yasuno Y. Polarization sensitive optical coherence tomography 2013; a review [Invited] [J]. ***Biomed Opt Express***, 2017, 8: 1838-1873.

[10] Baumann B. Polarization sensitive optical coherence tomography: A review of technology and applications [J]. ***Applied Sciences***, 2017, 7: 474.

[11] Siddiqui M, Nam A S, Tozburun S, et al. High-speed optical coherence tomography by circular interferometric ranging[J]. ***Nature Photonics***, 2018, 12: 111-116.

[12] Shu X, Beckmann L J, Zhang H F. Visible-light optical coherence tomography: a review [J]. ***Journal of Biomedical Optics***, 2017, 22: 121707.

[13] Povazay B, Apolonski A A, Unterhuber A, et al. Visible light optical coherence tomography [C]//Coherence Domain Optical Methods in Biomedical Science and Clinical Applications VI, International Society for Optics and Photonics, 2002, 4619: 90-94.

[14] Yi J, Chen S, Shu X, et al. Human retinal imaging using visible-light optical coherence tomography guided by scanning laser ophthalmoscopy [J]. ***Biomed Opt Express***, 2015, 6: 3701-3713.

[15] Kho A, Srinivasan V J. Compensating spatially dependent dispersion in visible light OCT [J]. ***Opt Lett***, 2019, 44: 775-778.

[16] Zhang T, Kho A M, Srinivasan V J. Improving visible light OCT of the human retina with rapid spectral shaping and axial tracking [J]. ***Biomed Opt Express***, 2019, 10: 2918-2931.

[17] Ju M J, Huang C, Wahl D J, et al. Visible light

sensorless adaptive optics for retinal structure and fluorescence imaging [J]. ***Opt Lett***, 2018, 43: 5162–5165.

[18] Coquoz S, Marchand P J, Bouwens A, et al. Label–free three–dimensional imaging of Caenorhabditis elegans with visible optical coherence microscopy [J]. ***PLOS ONE***, 2017, 12: e0181676.

[19] Marchand P J, Szlag D, Bouwens A, et al. In vivo high–resolution cortical imaging with extended–focus optical coherence microscopy in the visible–NIR wavelength range [J]. ***Journal of Biomedical Optics***, 2018, 23: 036012.

[20] Merkle C W. Chong S P, Kho A M, et al. Visible light optical coherence microscopy of the brain with isotropic femtoliter resolution in vivo [J]. ***Opt Lett***, 2018, 43: 198–201.

[21] Marchand P J, Bouwens A, Szlag D, et al. Visible spectrum extended–focus optical coherence microscopy for label–free sub–cellular tomography [J]. ***Biomed Opt Express***, 2017, 8: 3343–3359.

[22] Pi S, Camino A, Wei X, et al. Rodent retinal circulation organization and oxygen metabolism revealed by visible–light optical coherence tomography [J]. ***Biomed Opt Express***, 2018, 9: 5851–5862.

[23] Chen S, Yi J, Liu W, et al. Monte Carlo investigation of optical coherence tomography retinal oximetry [J]. ***IEEE Transactions on Biomedical Engineering***, 2015, 62: 2308–2315.

[24] Yi J, Wei Q, Liu W, et al. Visible–light optical coherence tomography for retinal oximetry[J]. ***Opt Lett***, 2013, 38: 1796–1798.

[25] Yi J, Backman V. Imaging a full set of optical scattering properties of biological tissue by inverse spectroscopic optical coherence tomography [J]. ***Opt Lett***, 2012, 37: 4443–4445.

[26] Faber D J, Aalders M C G, Mik E G, et al. Oxygen saturation–dependent absorption and scattering of blood [J]. ***Phys Rev Lett***, 2004, 93: 028102.

[27] Leitgeb R, Wojtkowski M, Kowalczyk A, et al. Spectral measurement of absorption by spectroscopic frequency–domain optical coherence tomography [J]. ***Opt Lett***, 2000, 25: 820–822.

[28] Morgner U, Drexler W, Kärtner F X, et al. Spectroscopic optical coherence tomography [J]. ***Opt Lett***, 2000, 25: 111–113.

[29] Yi J, Li X. Estimation of oxygen saturation from erythrocytes by high–resolution spectroscopic optical coherence tomography [J]. ***Opt Lett***, 2010, 35: 2094–2096.

[30] Robles F E, Chowdhury S, Wax A. Assessing hemoglobin concentration using spectroscopic optical coherence tomography for feasibility of tissue diagnostics[J]. ***Biomed Opt Express***, 2010, 1: 310–317.

[31] Robles F E, Wilson C, Grant G, et al. Molecular imaging true–colour spectroscopic optical coherence tomography[J]. ***Nature Photonics***, 2011, 5: 744–747.

[32] Yi J, Liu W, Chen S, et al. Visible light optical coherence tomography measures retinal oxygen metabolic response to systemic oxygenation [J]. ***Light: Science & Applications***, 2015, 4: e334.

[33] Chong S P, Merkle C W, Leahy C, et al. Cerebral metabolic rate of oxygen ($CMRO_2$) assessed by combined Doppler and spectroscopic OCT [J]. ***Biomed Opt Express***, 2015, 6: 3941–3951.

[34] Yi J, Chen S, Backman V, et al. In vivo functional microangiography by visible–light optical coherence tomography [J]. ***Biomed Opt Express***, 2014, 5: 3603–3612.

[35] Chen S, Yi J, Zhang H F. Measuring oxygen saturation in retinal and choroidal circulations in rats using visible light optical coherence tomography angiography [J]. ***Biomed Opt Express***, 2015, 6: 2840–2853.

[36] Liu R, Song W, Backman V, et al. Quantitative quality–control metrics for in vivo oximetry in small vessels by visible light optical coherence tomography angiography [J]. ***Biomed Opt Expres***s, 2019, 10: 465–486.

[37] Liu R, Winkelmann J A, Spicer G, et al. Single capillary oximetry and tissue ultrastructural sensing by dual–band dual–scan inverse spectroscopic optical coherence tomography[J]. ***Light: Science&Applications***, 2018, 7: 1–13.

[38] Liu W, Wang S, Soetikno B, et al. Increased retinal oxygen metabolism precedes microvascular alterations in type 1 diabetic mice [J]. ***Invest Ophthalmol Vis Sci***, 2017, 58: 981–989.

[39] Inner retinal oxygen metabolism in the 50/10 oxygen–induced retinopathy model | Scientific Reports. https://www.nature.com/articles/srep16752.

[40] Song W, Fu S, Song S, et al. Longitudinal detection of retinal alterations by visible and near–infrared optical

coherence tomography in a dexamethasone –induced ocular hypertension mouse model [J]. ***Neurophotonics***, 2019, 6: 041103.

[41] Pi S, Hormel T T, Wei X, et al. Monitoring retinal responses to acute intraocular pressure elevation in rats with visible light optical coherence tomography [J]. ***Neurophotonics***, 2019, 6: 041104.

[42] Soetikno B T, Shu X, Liu Q, et al. Optical coherence tomography angiography of retinal vascular occlusions produced by imaging–guided laser photocoagulation[J]. ***Biomed Opt Express***, 2017, 8: 3571–3582.

[43] Chen S, Liu Q, Shu X, et al. Imaging hemodynamic response after ischemic stroke in mouse cortex using visible–light optical coherence tomography [J]. ***Biomed Opt Express***, 2016, 7: 3377–3389.

[44] Chen S, Shu X, Nesper P L, et al. Retinal oximetry in humans using visible –light optical coherence tomography [Invited] [J]. ***Biomed Opt Express***, 2017, 8: 1415–1429.

[45] Boustany N N, Boppart S A, Backman V. Microscopic imaging and spectroscopy with scattered light [J]. ***Annual Review of Biomedical Engineering***, 2010, 12: 285–314.

[46] Barer R, Tkaczyk S. Refractive index of concentrated protein solutions[J]. ***Nature***, 1954, 173: 821–822.

[47] Yi J, Radosevich A J, Rogers J D, et al. Can OCT be sensitive to nanoscale structural alterations in biological tissue[J]. ***Opt Express***, 2013, 21: 9043–9059.

[48] Cherkezyan L, Capoglu I, Subramanian H, et al. Interferometric spectroscopy of scattered light can quantify the statistics of subdiffractional refractive –index fluctuations [J]. ***Phys Rev Lett***, 2013, 111: 033903.

[49] Radosevich A J, Yi J, Rogers J D, et al. Structural length –scale sensitivities of reflectance measurements in continuous random media under the Born approximation[J]. ***Opt Lett***, 2012, 37: 5220–5222.

[50] Hunter M, Backman V, Popescu G, et al. Tissue self–affinity and polarized light scattering in the born approximation: A new model for precancer detection[J]. ***Phys Rev Lett***, 2006, 97: 138102.

[51] Terry N G, Zhu Y, Rinehart M T, et al. Detection of dysplasia in Barrett′s ssophagus with in vivo depth–resolved nuclear morphology measurements [J]. ***Gastroenterology***, 2011, 140: 42–50.

[52] Qiu L, Pleskow D K, Chuttani R, et al. Multispectral scanning during endoscopy guides biopsy of dysplasia in Barrett′s esophagus [J]. ***Nature Medicine***, 2010, 16: 603–606.

[53] Mirabal Y N, Chang S K, Atkinson E N, et al. Reflectance spectroscopy for in vivo detection of cervical precancer [J]. ***Journal of Biomedical Optics***, 2002, 7: 587–595.

[54] Canpolat M, Akman–Karakas A, Gökhan–Ocak G A, et al. Diagnosis and demarcation of skin malignancy using elastic light single –scattering spectroscopy: A pilot study[J]. ***Dermatologic Surgery***, 2012, 38: 215–223.

[55] Lichtenegger A, Harper J D, Augustin M, et al. Spectroscopic imaging with spectral domain visible light optical coherence microscopy in Alzheimer& x02019; s disease brain samples [J]. ***Biomed Opt Express***, 2017, 8: 4007–4025.

[56] Harper D J, Konegger T, Augustin M, et al. Hyperspectral optical coherence tomography for in vivo visualization of melanin in the retinal pigment epithelium[J]. ***J Biophotonics***, 2019: e201900153.

[57] Harper D J, Augustin M, Lichtenegger A, et al. White light polarization sensitive optical coherence tomography for sub –micron axial resolution and spectroscopic contrast in the murine retina [J]. ***Biomed Opt Express***, 2018, 9: 2115–2129.

[58] Zhang X, Hu J, Knighton R W, et al. Dual –band spectral –domain optical coherence tomography for in vivo imaging the spectral contrasts of the retinal nerve fiber layer[J]. ***Opt Express***, 2011,19: 19653–19659.

[59] Chen S, Shu X, Yi J, et al. Dual–band optical coherence tomography using a single supercontinuum laser source [J]. ***Journal of Biomedical Optics***, 2016, 21: 066013.

[60] Song W, Zhou L, Zhang S, et al. Fiber –based visible and near infrared optical coherence tomography (vnOCT) enables quantitative elastic light scattering spectroscopy in human retina [J]. ***Biomed Opt Express***, 2018, 9: 3464–3480.

[61] Song W, Zhang L, Ness S, et al. Wavelength–dependent optical properties of melanosomes in retinal pigmented epithelium and their changes with melanin bleaching: a numerical study [J]. ***Biomed Opt Express***, 2017, 8: 3966–3980.